RSC Advances

ROYAL SOCIETY OF CHEMISTRY

www.rsc.org/advances

Cite this: DOI: 10.1039/c0xx00000x

www.rsc.org/xxxxxx

ARTICLE TYPE

Ligase-assisted, upconversion luminescence resonance energy transfer-based method for specific and sensitive detection of V600E mutation in BRAF gene

Peng Wang and Peng Zhang *

Received (in XXX, XXX) Xth XXXXXXXXX 20XX, Accepted Xth XXXXXXXXX 20XX
DOI: 10.1039/b000000x

The most common BRAF mutation, V600E, accounts for a variety of cancers. Here we report a highly specific and sensitive method for the detection of the V600E mutation. The detection scheme is based on luminescence resonance energy transfer (LRET) between upconversion nanoparticles (UCNPs) and an intercalating dye, SYBR Green I. Target DNA serves as the template for two DNA probes, one of them covalently attached to UCNPs, to be ligated into a hairpin-forming DNA strand, which brings SYBR Green I close to the upconversion nanoparticles. The number of the resulting DNA strand is amplified through thermal cycling. The degree of LRET is correlated to the amount of the initial DNA targets. Factors affecting the detection specificity and sensitivity, including ligation temperature, amount of ligase, and number of thermal cycles, have been investigated to optimize the performance of the detection method. The method can easily differentiate the V600E mutation from the wild-type sequence with a mutant-to-wild-type ratio of 1:1000. A detection limit of 1 femtomole BRAF V600E mutation is achieved.

Introduction

BRAF mutations are known as malignant drivers in a number of cancers [1,2], such as melanoma, papillary thyroid cancers, non-small cell lung cancer [3,4]. Activating mutation of BRAF is found to usually occur in a hotspot of amino acid position 600 by a missense substitution of valine by glutamic acid, known as the BRAF V600E mutation [5]. Although combination chemotherapy has been attempted to patients suffering cancers with this mutation, it has yet to prove to significantly improve the survival of patients. Furthermore, traditional chemotherapeutic methods often result in significant systemic cytotoxicity [6-8]. Thus, detection of the BRAF V600E mutation has important genetic, prognostic, and therapeutic implications for patients with these cancers. Currently, detection of BRAF mutations relies on molecular methods, including conventional sequencing, pyrosequencing, or allele-specific polymerase chain reaction (PCR) with melting curve analysis. Recently, a monoclonal mouse antibody specifically detecting the mutated (V600E) BRAF protein in formalin-fixed, paraffin embedded tissues has been described and may represent a practical tool for screening [9-11]. Still, these methods either require specialized equipment [12], employ conceptually complex processes that may be difficult to troubleshoot [13], or require restriction enzyme digestion [14].

In recent studies, there have been growing interests in developing luminescence resonance energy transfer (LRET) based detection schemes [15-19], a process of energy transfer between a donor (typically nanoparticles) and an acceptor (quenchers or dyes) [20]. Upconversion nanoparticles (UCNPs) can emit higher-energy visible photons after absorbing lower-energy infrared photons. Compared to the commonly used down-conversion fluorophores or quantum dots, UCNPs possess some unique features, including sharp emission bands, long luminescence lifetimes, superior photostability, the near-absence of autofluorescence resulting in a high signal-to-background ratio, and the deep tissue penetration by near-IR excitation. There have been a number of reports on detection methods based on UCNPs with good specificity and sensitivity [17,19,21,22]. Yet few of them involved targets directly associated with actual diseases. We have previously reported a proof-of-concept study that integrates the DNA ligation into a UCNP-based detection method [23]. Herein we build upon that study to demonstrate a highly specific and sensitive method for the detection of BRAF V600E mutation. Several factors affecting the detection specificity and sensitivity have been considered and investigated to optimize the performance and feasibility of the detection scheme for use in clinical applications. To our knowledge, this is the first report on detecting BRAF V600E mutation using UCNPs and ligation reaction.

Experimental

Chemicals and materials

$Y(NO_3)_3•6H_2O$, $Yb(NO_3)_3•5H_2O$, $Tm(NO_3)_3•5H_2O$, $NaNO_3$, NH_4F, polyacrylic acid (PAA, MW ~15000), polyacrylic acid

(PAA, MW ~1800), and ethylenediaminetetraacetic acid (EDTA) were from Sigma (St. Louis, MO). 1-Ethyl-3-[3-dimethylamonopropyl]carbodiimide hydrochloride (EDC), N-hydroxysulfosuccinimide (NHS) and ethylene glycol (EG) were from Thermo Scientific (Rockford, IL). SYBR Green I was from Life Technology (Carlsbad, CA). DNA strands were from IDT DNA (Coralville, IA). Taqligase® and 10× Taqligase® reaction buffer were purchased from New England BioLabs. The melting points of various DNA strands under the experimental conditions were calculated using the OligoAnalyzer program available at the vendor's website (www.idtdna.com).

All sequences of DNA probes and targets used in this study are listed in Table 1. The DNA targets are DNA_tar (44mer), which is a section of the BRAF V600E containing the A->T mutation as highlighted in bold red, and DNA_mis (44mer), which is the same section of normal BRAF gene (wild-type). Two single-stranded DNA probes are used: DNA_1 (33mer, amine-modified at the 5'-end) and DNA_2 (22mer, phosphorylated at the 5'-end).

Table 1. Probes and target DNA sequences used in this study.

DNA_1	3'- GAG ACA TCG ATC TGG TTT TAG T CTC ACC CAG GG - AmMC6 - 5'
DNA_2	3'- C CCT GGG TGA GGT AGC TCT AAA - pho - 5'
DNA_tar	5'- G GGA CCC ACT CCA TCG AGA TTT CTC TGT AGC TAG ACC AAA ATC A -3'
DNA_mis	5'- G GGA CCC ACT CCA TCG AGA TTT CAC TGT AGC TAG ACC AAA ATC A -3'

Synthesis of $NaYF_4$;Yb^{3+},Tm^{3+}upconversion nanoparticles

PAA (MW~15000, 0.225 g), PAA (MW~1800, 0.075 g), $NaNO_3$ (34 mg), $Y(NO_3)_3$•$6H_2O$ (61.2 mg), $Yb(NO_3)_3$•$5H_2O$ (17.7 mg), and $Tm(NO_3)_3$•$5H_2O$ (0.5 mg) were mixed into 3 ml of EG, using vortex and sonicator to make the mixture homogenous (Solution A). Separately, 0.03 g of NH_4F was dispersed into 2 mL of EG in a Teflon container (Solution B). Solution A was added into Solution B drop wise under stirring. The Teflon container was then placed in a sealed stainless-steel capsule, and heated in an oven at 220 °C for 24 hr. The resulting solution was clear with light yellow in color. The nanoparticles were collected by centrifugation at 15,000 rpm for 1 hr to remove the supernatant. They were washed 3 times by ethanol and twice by DI water before storage for later use.

Conjugation of DNA_1 to UCNPs

Three ml of washed UCNP aqueous solution was treated with 10 µL of EDC (0.2 M) and 10 µL of NHS (0.05 M) for 5 min under stirring at 600 rpm. Next, 100 µL of 100 µM DNA_1 was added into the mixture and stirred at 600 rpm overnight. The resulting nanoparticles were washed 3 times by DI water, before dispersed in 1 mL of DI water.

Determination of conjugation yield of DNA_1 to UCNPs

The amount of DNA_1 conjugated to the UCNPs was determined experimentally following procedures described previously [23]. A standardization curve of DNA_1 with SYBR Green I solution was first obtained under different DNA_1concentrations (0, 0.1, 0.25, 0.5, 1.0, 2.5, 5 µM). In these measurements, SYBR Green I was excited at 480 nm using a Xenon lamp with 1-mm slit width, and the emission intensity at 530-535 nm was measured. Then 100 µL of DNA_1-conjugated UCNP working solution was diluted 10 times, and incubated with the same amount of SYBR Green I solution. The fluorescence intensity of the mixture at 530-535 nm was again measured while excited at 480 nm. The concentration of DNA_1 in the diluted solution was calculated based on the standardization curve, and the yield of the conjugation between UCNPs and DNA_1 determined.

DNA Ligation and hairpin loop amplification through thermal cycling

Thirty µL of DNA_1 conjugated UCNP solution was added into 10 µL of 10× ligase reaction buffer, 1 µL of ligase (Tagligase®) and 20 µL of 1 µM DNA_2 with different volumes of 0.1 µM target DNA. The mixture was brought to a total volume of 100 µL using buffer, and treated in 85 °C for 30 second. The solution was then cooled down to a lower temperature (54, 57, or 60 °C as discussed later) and maintained for 3 min before being heated up to 85 °C again. This thermal cycle was repeated 80 times unless specified otherwise in a thermal cycler. By the end of the cycling, EDTA solution was quickly added to the mixture to stop further ligation. Subsequently, the nanoparticles were centrifuged and washed. In the figures shown below, control sample refers to replacing the DNA target with the same amount of DI water. Match sample refers to DNA_tar, and mismatch to DNA_mis.

Luminescence measurement at 980 nm excitation

Five hundred µL of UCNP-DNA_1 mixture after the respective thermal treatment was mixed with 500 µL of 10 µM SYBR Green I solution in 10 mM sodium phosphate buffer (pH 7.8). The solution was put in a quartz cuvette. Emission spectra were collected on a spectrofluorometer (PTI, NJ), which is equipped with an external 980-nm laser (Laserglow Technology, Canada) as the excitation source. Slit width was set at 2.0 mm. When calculating the ratio of I_{533}/I_{477}, I_{533} is the integrated area between 530 to 535 nm and I_{477} is that between 475 to 480 nm.

TEM measurement

TEM samples were prepared by air-drying a drop of sample solution on a Formvar-covered carbon-coated copper grid (EMS, PA). TEM images were collected using a Biotwin 12 transmission electron microscope (FEI, Netherlands). The images were analyzed by ImageJ software.

Results and discussion

The upconversion nanoparticles used in this work are Yb^{3+}/Tm^{3+} co-doped $NaYF_4$ nanoparticles. The UCNPs are synthesized by a hydrothermal method similar to what was described previously [23,24]. UCNPs synthesized by this method are bright when excited by a 980 nm laser, with a strong emission peak at ~477 nm. Transmission electron microscopy (TEM) image of the UCNPs (Figure 1) shows that they are fairly monodispersed with diameter of 190 ± 10 nm after analyzing a total of 60 particles. In addition, they are highly dispersible in water because of the

abundant carboxylic acid groups on the nanoparticle surface. Note that these upconversion nanoparticles have slight different size distribution compared to those used in our previous reports [23,24], because they are synthesized with two types of PAA and the rare earth salts are nitrates instead of chlorides used previously.

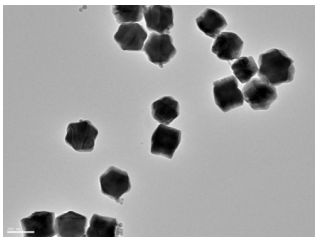

Figure 1. TEM images of $NaYF_4$; Yb^{3+},Tm^{3+} upconversion nanoparticles. Scale bar: 200 nm.

DNA_1 is covalently conjugated to the UCNPs through the widely used EDC/NHS method. The amount of the conjugated DNA_1 to the UCNPs was determined experimentally. SYBR Green I emits weak fluorescence in the presence of single strand DNA, and can be used to quantify the amount of DNA_1 on the UCNP surface. The standardization curve of DNA_1 in 5 μM SYBR Green I solution was obtained with different concentrations of DNA_1 (Figure 2), showing a linear relationship between the fluorescence intensity of SYBR Green I at 533 nm and the concentration of DNA_1 (in μM). The fluorescence intensity of 5 μM SYBR Green I solution in the presence of 10× diluted DNA_1-conjugated UCNPs was also measured. Based on the standardization curve, we calculated that the concentration of DNA_1 in the working solution of DNA_1-conjugated UCNPs was 0.27 μM, corresponding to a conjugation yield of ~27% between UCNPs and DNA_1. We did not attempt to optimize the concentration of DNA_1 conjugated to UCNPs in this study.

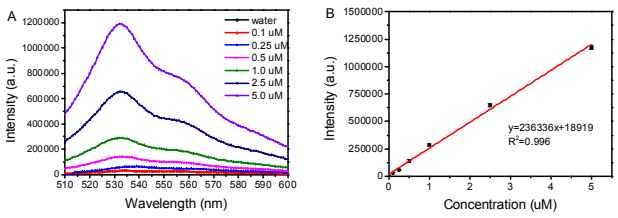

Figure 2. (A) SYBR Green I fluorescence spectra excited at 480 nm with different concentrations of DNA_1. (B) Plot of I_{533} vs. DNA_1 concentration.

The detection scheme is illustrated in Figure 3. The underlying principle is LRET between the UCNPs and the intercalating dye, SYBR Green I. Two single-stranded DNA strands are each complementary to a juxtaposed section of the target DNA. One of the DNA probes is conjugated to the UCNPs. The design of the probe sequences includes a segment in each probe (underlined sections in Table 1) so that, when they are joined into one long DNA strand, a hairpin loop structure will be formed under ambient temperature. In the presence of the target DNA and ligase, ligation takes place between the two probes resulting in the formation of a hairpin-forming DNA strand with the sequence of 3'- C CCT GGG TGA GGT AGC TCT AAAGAG ACA TCG ATC TGG TTT TAG T CTC ACC CAG GG- 5', where the underlined bases indicate the stem portion of the hairpin structure. The number of the hairpin-forming DNA strands formed on the UCNP surface is amplified through thermal cycling between probe ligation at a lower temperature and DNA dehybridization at a higher temperature. In the presence of the mismatch target, ligation would not occur thus no hairpin-forming strands are formed on the UCNP surface.

The DNA_mis sequence is only one base different from the DNA_tar sequence. In our previous study [24], we found that the difference in signal between the match and mismatch targets was the largest when the mismatched base was at the penultimate 3'-position near the ligation point, leading to the best specificity of detection. Accordingly, DNA_1 probe is so designed that the mismatched base is located at its penultimate 3'-position. The nanoparticles are washed after the thermal cycling, before mixing with the intercalating dye, SYBR Green I. SYBR Green I, which has an excitation band overlapping with the UCNPs emission, are trapped in the stem portion of the hairpin-forming strand. Upon excitation at 980 nm, luminescence resonance energy transfer (LRET) would occur between the UCNPs and the nearby intercalated SYBR Green I. By monitoring the ratio of SYBR Green I emission at ~533 nm and UCNP emission at ~477 nm, we can determine whether ligation takes place between the two DNA probes. Since the target DNA serves as a template for the ligation, the ratio of I_{533}/I_{477} is used to indicate the presence of the target DNA. The ratiometric measurement would self-calibrate the possible variation in the amount of UCNPs used among different runs.

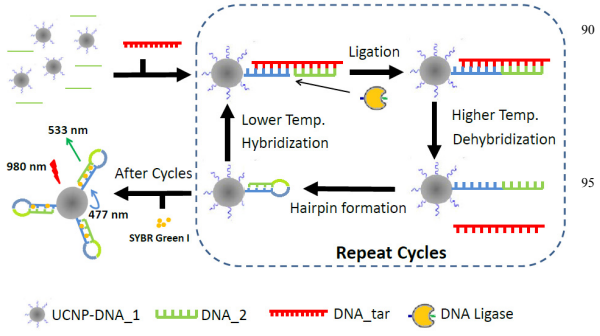

Figure 3. Illustration of the ligase-assisted DNA detection scheme based on UCNPs. For DNA match target, ligation occurs and thermal cycling would increase the number of the hairpin structure formed on the UCNP surface.

This detection scheme displays the following features: high signal-to-noise ratio and high fidelity. The luminescence measurements are carried out under excitation of a 980-nm laser,

which avoids any autofluorescence or cross-excitation. The background signal is essentially the baseline of the instrument. Thus even weak signals can have very high S/N ratios. Any free SYBR Green I in the solution would not affect the detection, as only those intercalated SYBR Green I near the UCNP surface participate in the LRET. The initial target DNA strands serve as template for all ligation steps, maintaining the high fidelity of the ligation, while linearly amplifying the number of hairpin-forming DNA strands on the UCNPs. Accordingly, the detected signal is linearly amplified with the increase in the number of thermal cycles. These features should lead to high specificity and sensitivity of the detection. As shown in Figure 4, in the presence of DNA_tar, the 477-nm band decreases markedly while the 533-nm band increases slightly due to the LRET between the UCNPs and SYBR Green I. Yet with DNA_mis as target, the spectrum is essentially the same as that of control, indicating very little ligation occurs in the presence of DNA_mis.

We further optimize several factors that affect the performance of this detection scheme. In principle, ligation temperature should affect specificity, while the number of thermal cycles and, possibly, the amount of ligase affect the sensitivity. As shown in Figure 4, the increase of the amount of Taqligase added does not appear to increase the I_{533}/I_{477} ratio, indicating that 10 units of ligase is sufficient for the ligation reaction under the experimental conditions. Thus, we opted to use 10 units of ligase in later runs.

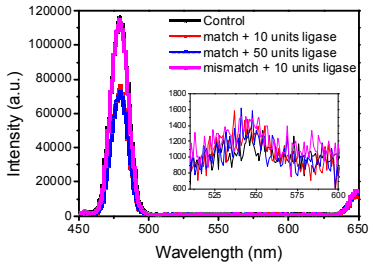

Figure 4. Emission spectra of UCNPs after 40 thermal cycles at ligation temperature of 57 °C with 2 pmol DNA targets and different amounts of Taqligase. The inserts show the 10x amplification of a portion of the spectra.

Ligation temperature is expected to have a major impact on the performance of the detection. On one hand, if the ligation temperature is low, hybridization between the target and probes is more efficient, leading to higher ligation efficiency with the same number of cycles and thus higher sensitivity. However, both DNA_tar and DNA_mis would hybridize with the two probes, reducing the specificity. On the other hand, higher ligation temperature improves the specificity, as only the matched target would be able to hybridize with the probes and allow the ligation to occur. Yet if the ligation temperature is set too high, only small amounts of DNA_tar would hybridize with the probes, which would lead to low sensitivity. Therefore it is important to select a sufficiently low ligation temperature while simultaneously achieving high differentiation between the two targets. The melting point of DNA_1 under the experimental conditions is 57 °C. Therefore three different ligation temperatures, 54, 57, and 60 °C, were tested, with results shown in Figure 5. Notice the similarity between runs of control and mismatch sample at higher ligation temperature. Since ligation at 60 °C does not seem to further improve the detection specificity as compared with ligation at 57 °C, we opted to set the ligation temperature of 57 °C in the later experiments to determine the detection sensitivity of DNA_tar.

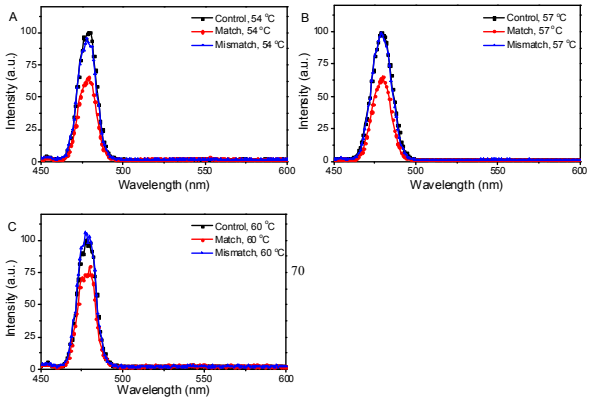

Figure 5. Emission spectra of UCNPs after 40 thermal cycles with 2 pmol DNA targets and 10 units of Taqligase at different ligation temperatures (A) 54 °C, (B) 57 °C, (C) 60 °C.

The number of thermal cycles is expected to affect the number of hairpin-forming DNA strands on the UCNP surface, and subsequently the detection sensitivity. As shown in Figure 6A, we have tested different numbers of thermal cycles, ranging from 10 to 160. The I_{533}/I_{477} ratio is plotted vs. the number of cycles in Figure 6B. The curve appears to approach a plateau, suggesting that, while it is possible to improve the detection sensitivity by increasing the number of thermal cycles, the effectiveness in improving the sensitivity decreases as the cycle number increases. Based on the consideration of sensitivity and total operation time, we decided to use 80 cycles in most measurements.

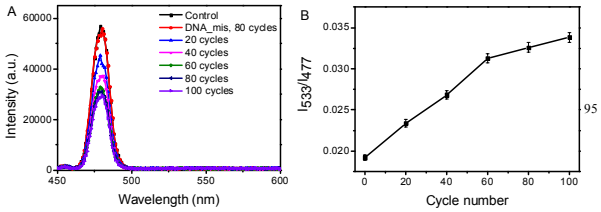

Figure 6. (A) Emission spectra of UCNPs after different cycles in the presence of 1 pmol DNA targets and 10 units of Taqligase at ligation temperature of 57 °C. (B) I_{533}/I_{477} vs. number of cycles.

These results combine to support the notion that the detection sensitivity is determined largely by the number of thermal cycles and to a small extent by the amount of ligases used. Under the condition of 10 units Taqligase and 80 cycles, we carried out a series of experiments with different amounts of DNA_tar. The results in Figure 7 show that 1 femtomole of DNA_tar can be readily detected. The linear range from 0.1 to 2.0 pmol can be

used to quantify the DNA_tar concentration. Also notice the gap between 0 and 1 femtomole DNA_tar in the inset of Figure 7B, which implies that the sensitivity can be further improved.

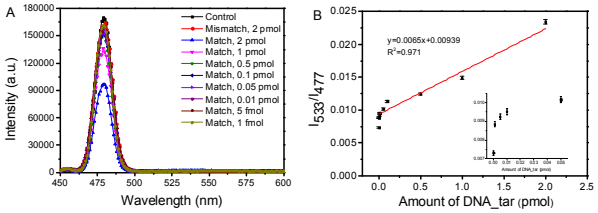

Figure 7. (A) Emission spectra of UCNPs under 980 nm excitation after 80 thermal cycles at ligation temperature of 57°C in the presence of different amounts of DNA_tar. (B) I_{533}/I_{477} vs. amount of DNA_tar. The insert shows I_{533}/I_{477} vs. amount of DNA_tar from 0 to 0.1 pmol. Error bars are based on the results of five measurements for each data point.

In clinical settings, the mutated DNA strand is most likely present with a large amount of the wild-type strands. Thus it is important to check out whether the scheme can detect DNA_tar in the presence of DNA_mis. Figure 8 shows the results when mixture of different ratios of DNA_tar and DNA_mis was used as targets. The difference in the emission spectra from the control is significant for mixtures of DNA_tar/DNA_mis ratio down to 0.1% as confirmed statistically by the t-test. By plotting I_{533}/I_{477} vs. DNA_tar/DNA_mis, a mutant-to-wild-type ratio of 1:1000 can be achieved for the detection. This indicates great potential of the detection scheme for clinical use.

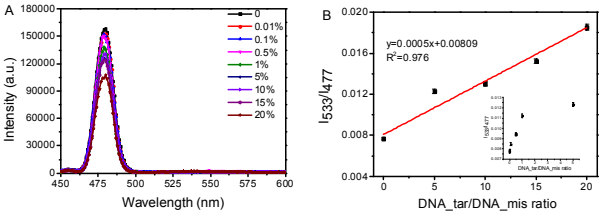

Figure 8. (A) Emission spectra of UCNPs after 80 cycles in the presence of mixture of DNA targets (total DNA of 2 pmol) with different DNA_tar/DNA_mis ratios and 10 units of Taqligase at the ligation temperature of 57 °C. (B) I_{533}/I_{477} vs. ratio of DNA_tar to DNA_mis. The inserts show I_{533}/I_{477} vs. ratio of DNA_tar to DNA_mis from 0 to 5%. The error bars are based on the results of five measurements for each data point.

Conclusions

In summary, we report a ligation-based, signal amplifiable method to detect BRAF V600E mutation using upconversion nanoparticles. The method can readily differentiate the mutated strand in the matrix containing abundant wild-type strands, down to a mutant-to-wild-type ratio of 1:1000. A detection limit of 1 femtomole BRAF V600E mutation was achieved. Factors affecting the detection specificity and sensitivity are thoroughly investigated. Results indicate that ligation temperature can be adjusted to achieve high detection specificity, while cycle number helps improve the detection sensitivity. The detection scheme has the potential for clinical applications and can be adopted for detection of other DNA mutants.

Acknowledgement

Support from the Natural Science Foundation (CBET-1065633) is gratefully acknowledged.

Notes and references

* *Department of Chemistry, University of Cincinnati, Cincinnati, OH 45221. E-mail: peng.zhang@uc.edu*

† Electronic Supplementary Information (ESI) available: [details of any supplementary information available should be included here]. See DOI: 10.1039/b000000x/

1 Davies H, Bignell GR, Cox C, Stephens P, Edkins S, Clegg S, et al. *Nature* **2002**, *417*, 949.
2 Wan PT, Garnett MJ, Roe SM, Lee S, Niculescu-Duvaz D, Good VM, et al. *Cell* **2004,** *116*, 855.
3 Platz A, Egyhazi S, Ringborg U, Hansson J. *Mol Oncol* **2008**, *1*, 395.
4 Greaves WO, Verma S, Patel KP, Davies MA, Barkoh BA, Galbincea J.M. *J Mol Diagn* **2013**, *15*, 220.
5 Vaughn CP, Zobell SD, Furtado LV, Baker CL, Samowitz WS. *Genes Chromosomes Cancer* **2011**, *50*, 307.
6 Atkins MB, Hsu J, Lee S, Cohen GI, Flaherty LE, et al. *J Clin Oncol* **2008**, *26*, 5748.
7 Algazi AP, Weber JS, Andrews SC, et al. *Br J Cancer* **2012**, *106*, 85.
8 Jiang G, Li RH, Sun C, Jia HY, Lei TC, Liu YQ. *Tumour Biol* **2014**, *35*, 315.
9 Capper D, Preusser M, Habel A, et al. *Acta Neuropathol* **2011**, *122*, 11.
10 Andrulis M, Penzel R, Weichert W, von Deimling A, Capper D. *Am J Surg Pathol* **2012,** *36*, 1796.
11 Koperek O, Kornauth C, Capper D, et al. *Am J Surg Pathol* **2012**, *36*, 844.
12 Thomas RK, Greulich H, Yuza Y, Lee JC, et al. *Cold Spring Harb Symp Quant Biol* **2005**, *70*, 73.
13 Hoshi K, Takakura H, Mitani Y, Tatsumi K, et al. *Clin Cancer Res* **2007,** *13*, 4974.
14 Asano H, Toyooka S, Tokumo M, Ichimura K, et al. *Clin Cancer Res* **2006**, *12*, 43.
15 Zhang P, Rogelj S, Nguyen K, Wheeler D. *J Am Chem Soc* **2006,** *128*, 12410.
16 Guo Y, Kumar M, Zhang P. *Chem Mater* **2007,** *19*, 6071.
17 Zhang P, Steelant W, Kumar M, Scholfield M. *J Am Chem Soc* **2007**, *129*, 4526.
18 Wang F, Liu X. *Chem Soc Rev* **2009**, *38*, 976.
19 Kumar M, Zhang P. *Biosens Bioelectron* **2010,** *25*, 2431.
20 Andrews DL. *Chem Phys* **1989**, *135*, 195.
21 Kumar M, Zhang P. *Langmuir* **2009**, 25(11), 6024-7.
22 Kumar M, Guo Y, Zhang P. *Biosens. Bioelectron*. **2009**, 24, 1522.
23 Wang P, Ahmadov TO, Lee C, Zhang P. *RSC Adv* **2013,** *3*, 16326.
24 Wang P, Joshi P, Alazemi A, Zhang P. *Biosens Bioelectron* **2014,** *24*, 120.

Ligase-assisted, upconversion luminescence resonance energy transfer-based method for specific and sensitive detection of V600E mutation in BRAF gene

Peng Wang, Peng Zhang*

Department of Chemistry, University of Cincinnati, Cincinnati, Ohio, 45221

Table Content Used Only:

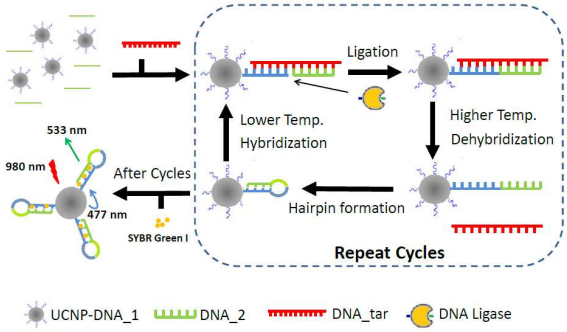

Text: We report a specific and sensitive detection of BRAF V600E mutation based on a ligase-assisted signal-amplifiable scheme using upconversion nanoparticles.